

https://doi.org/10.1070/QEL16298

Laser-induced boiling of biological liquids in medical technologies

V.M. Chudnovskii, V.I. Yusupov, A.V. Dydykin, V.I. Nevozhai,
A.Yu. Kisilev, S.A. Zhukov, V.N. Bagratashvili

Abstract. **Using optical and acoustic methods we study thermal and transport processes related to the boiling of biological liquids under the action of continuous-wave laser radiation having moderate power (1–10 W) in the near-IR range (0.97–1.94 μm) . These processes are investigated in the course of a few particular clinical procedures aimed at the modification and removal of pathological tissues (veins, mammary gland cyst, Baker's cyst) and tissue regeneration (intervertebral discs). In the proposed approach, the modification and destruction of biotissues are due to the fast delivery of heat by two-phase jet flows, formed in the course of liquid boiling, rather than the direct laser heating. This provides the high rate of heat delivery to the pathological biotissue, avoiding its overheating (the temperature higher than 100 °C) and undesired heating of adjacent tissues. Two main regimes of laser-induced boiling near the optical fibre tip were revealed, namely, the heterogeneous jet boiling (arising when the fibre with a blackened tip is used) and the homogeneous boiling (with the radiation absorbed in the liquid volume). Both studied regimes allow one to obtain high specific heat flows, and the domination of one of the boiling regimes is determined by the presence of absorbing coating on the fibre tip, the tissue type, as well as by its shape (e.g., the presence of channels or cavities in the tissue). It is established that the heterogeneous jet boiling at the fibre tip corresponds to the regime of superintensive bubble boiling.**

Keywords: *laser medical technologies, fibre lasers, optical fibre, laser-induced boiling, biological liquid, vein, intervertebral disc, cyst.*

1. Introduction

Progress in quantum electronics and laser engineering has lead to the appearance of a number of new laser medical technologies (in otolaryngology, neurosurgery, orthopaedics, phlebology, cosmetology, etc.) [1–6], where compact and reliable fibre lasers with moderate power (1–10W) generating continuous-wave radiation in the near-IR range are used [7]. Using them, a number of novel medical techniques have been implemented. Among the variety of laser-stimulated thermal processes taking place under the exposure of biotissues to laser radiation, an important role is played by the processes of biological liquid boiling [8, 9] and the boiling-induced hydrodynamic processes [10–13].

Boiling is a process of intense vaporisation inside a liquid [14–16]. One should distinguish between the heterogeneous boiling that occurs on the surface of a heater, to which the heat is supplied from outside, and the homogeneous boiling that occurs in the volume of an overheated liquid. Intense convective heat flows and the expenditures for the latent vaporisation heat make the boiling an efficient way of heat transfer, widely used in different technical devices for cooling [16]. The most intense heat flows appear when the boiling is initiated in a liquid below the saturation temperature (subcooled boiling) [14–19]. In contrast to the developed bubble boiling [14–16], the subcooled boiling is accompanied not only by the growth of vapour-gas bubbles, but also with their collapse. This leads to the known effects, such as the superintensive bubble boiling [17], microbubble boiling [19], thermocavitation (the explosive growth and cavitation collapse of vapour cavities) [20–24], hydrodynamic and thermoacoustic autooscillations in resonators [25, 26].

In some medical technologies the thermal flows from a heater, related to the boiling of a biological liquid are used to heat biotissues and thermally destroy pathological tissues [8–10]. The boiling of a biological liquid, an aqueous solution with the saturation temperature ~100 °C, leads to the heating and destruction of biological components. The laser heating used in some modern percutaneous technologies [2–7, 10] is rather convenient for this purpose. In these technologies, the laser energy is delivered to the tissue through a silica optical fibre. If the laser radiation is well absorbed in the biological liquid or water-saturated biotissue, it can initiate its homogeneous boiling [27]. The boiling leads to fast heating of the entire volume of the liquid, in which the vapour-gas bubbles collapse [25, 26]. In such regime the laser heating (hyperthermia) of bulk pathological masses is efficient [28].

If the optical fibre tip is coated with an absorbing substance (blackened), then under the exposure to radiation this layer is heated to high temperatures [11, 27, 29, 30]. The contact with biological liquids leads to their heterogeneous boiling at the heated tip of the optical fibre, which under certain conditions is accompanied by the formation of two-phase flows. Directed jet flows can provide fast heat transfer from the heated tip of the fibre to the biotissue, e.g., the cyst shell

V.M. Chudnovskii V.I. Il'ichev Pacific Oceanology Institute, Far Eastern Branch, Russian Academy of Sciences, ul. Baltiyskaya 43, 690041 Vladivostok, Russia;
V.I. Yusupov, V.N. Bagratashvili Institute of Photon Technologies, Federal Scientific Research Centre 'Crystallography and Photonics', Russian Academy of Sciences, ul. Pionerskaya 2, Troitsk, 108840 Moscow, Russia; e-mail: iouss@yandex.ru;
A.V. Dydykin OOO 'Prosto laboratoriya' Clinic, Block B, 8, 665824 Angarsk, Irkutsk region, Russia;
V.I. Nevozhai Pacific State Medical University, prosp. Ostryakova 2, 690002 Vladivostok, Russia;
A.Yu. Kisilev Far Eastern Federal University, ul. Sukhanova 8, 690090 Vladivostok, Russia;
S.A. Zhukov Institute of Problems of Chemical Physics, Russian Academy of Science, prosp. Akad. Semenova 1, 142432 Chernogolovka, Moscow region, Russia

Received 2 February 2017; revision received 10 March 2017
Kvantovaya Elektronika **47** (4) 361–370 (2017)
Translated by V.L. Derbov

[7, 31, 32] or the inner shell of veins [10, 33] through the volume of cyst fluid or blood filling the vein. In this regime the temperature of the pathological tissue is increased to the temperature of the jet flow, which leads to its thermal destruction, while the temperature of the entire volume of the liquid is not increased that much. Thus, different regimes of the biological liquid boiling allow the implementation of different approaches to the laser treatment of pathological structures, comprising the volumes filled with a liquid.

Both regimes of laser-induced boiling of a liquid (homogeneous and heterogeneous) are known to be accompanied by the generation of broadband acoustic waves [21, 22, 34] which under the conditions of resonance coupling can give rise to the resonancely amplified autooscillations [25, 26]. As to the resonators inside the organism (intervertebral discs, hollow bones, sinuses, etc.), such autooscillations can lead to important results, i.e., the destruction of intervertebral disc herniation [2, 4, 12, 13], sanitation of medullary canal in the laser surgical treatment of osteomyelitis [5], and the triggering of the biotissue regeneration process [12, 35, 36].

The development of novel laser medical technologies makes the study of boiling effects in different systems very urgent. The laser-induced hydrodynamic processes can be efficiently controlled using remote acoustic methods [21, 22, 34] and rapid video recording [27].

In this paper, we consider the effects of laser-induced boiling of water and biological liquids, heated below the saturation temperature, playing an important role in a number of particular medical technologies of percutaneous treatment using the moderate-power fibre lasers. These effects are used in the cases of endovasal laser ablation (EVLA) of the great saphenous vein when treating the chronic venous insufficiency, the pathologically changed intervertebral disc, the mammary gland cyst, as well as a Baker's cyst (a popliteal cyst).

2. Materials and methods

The processes of laser-induced boiling were studied in water and in biological tissues (Fig. 1) both *in vitro* and *in vivo* during the execution of a few clinical procedures of laser percutaneous treatment of the above pathologies [2, 12, 31, 33, 37]. In the *in vitro* experiments modelling the percutaneous laser technology of the osteochondrosis treatment [2] the materials for the study were the whole spinal motion segments with intervertebral discs (Fig. 1b) extracted from six patients that died from somatic diseases at the age from 45 to 75.

As a source of radiation we used a cw laser (IRE-Polus, Russia) having the moderate power (1–10 W) and the wavelength λ = 0.97, 1.56, or 1.94 μm. The radiation from the laser was transmitted via the silica fibre with the core diameter of 400 μm. For the chosen wavelengths, the absorption coefficients in water are essentially different: 0.47 cm^{-1} for λ = 0.97 μm, 10 cm^{-1} for λ = 1.56 μm, and 92 cm^{-1} for λ = 1.94 μm [38]. The studies were carried out in two regimes of laser impact: with the absorbing coating on the fibre tip and without it. The absorbing coating was deposited by contacting (during ~1 s) the fibre tip with a wooden bar at $P \sim 3$ W, which lead to stable covering of the tip with a layer of amorphous carbon [27].

For the EVLA procedure, we used an optical fibre with a tip having a diameter of 3.7 mm without an absorbing coating which provided the radial exit of radiation. The fibre was connected to a Ceralas E15 Elves diode laser (Germany) with the wavelength λ = 1.47 μm, located in the region of the local maximum of water absorption [38] (the absorption coefficient 30 cm^{-1}).

The detection of acoustic signals was performed in the cuvette with the dimensions 24 × 40 × 24 cm filled with water at room temperature, in which the operating tip of the laser fibre was submerged. At a distance of ~1 cm from the tip, at the side of the fibre, a broadband hydrophone 8103 (Bruel&Kjaer, Danmark) having a detector sensitivity band (±2 dB) 0.1 Hz–180 kHz and a needly hydrophone (Precision Acoustics, Great Britain) having a diameter of 1 mm and a detector sensitivity band (±4 dB) 200 kHz–15 MHz with a preamplifier were installed. The acoustic signals from the hydrophones were recorded using a GDS 72304 oscilloscope (GW Instek) with a transmission bandwidth 300 MGz. The energy of the acoustic signal was estimated assuming the sphericity of the acoustic wave, and the pressure was recalculated to the distance 1 mm from the source.

To perform the acoustic measurements *in vitro* the spinal motion segment was placed in a basin with water. The hydrophone 8103 was installed at a distance of 1 cm from the studied object. The clinical acoustic measurements were executed in the course of percutaneous laser treatment of the pathologically changed intervertebral disc [2, 12] and EVLA of great saphenous vein in the course of treatment of the chronic venous insufficiency [33].

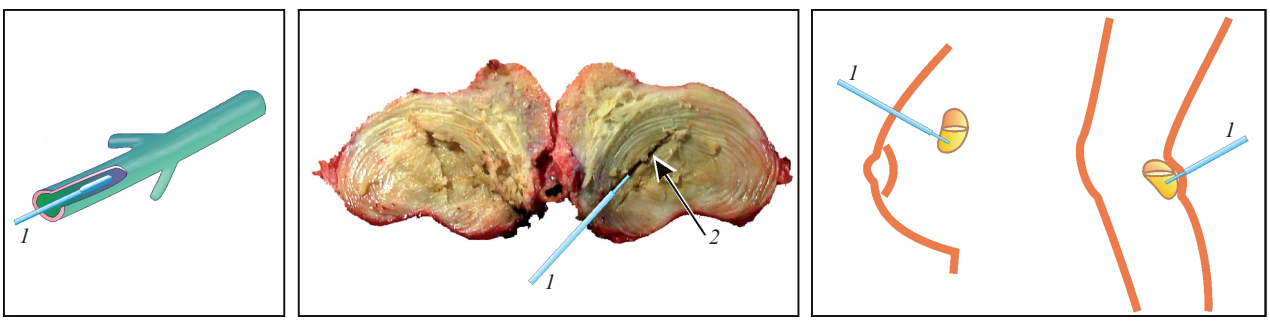

Figure 1. (a, c) Schematic and (b) photographic images of the objects, in which under the action of cw laser radiation different regimes of boiling of biological liquids are implemented: (a) vein, (b) section of intervertebral disc of the spinal motion segment with laser channel, (c) mammary gland cyst (left) and Baker's cyst (right); (*1*) laser fibre, (*2*) laser channel.

The *in vivo* studies were carried out using a special acoustic detector and preamplifier with the band 0.3–15 kHz. The detector was fabricated using a standard stethoscope head, in which a miniature electret capacitor microphone was mounted. In the treatment of the pathologically changed intervertebral disc, the acoustic detector lubricated with gel along the perimeter was firmly pressed to the patient's skin in the disc projection and was fixed with adhesive tape. The *in vivo* and *in vitro* manipulations with the intervertebral discs were alike. They were carried out with pauses and the total time was 7 min.

According to the technique of Ref. [2], in the nucleus pulposis of the intervertebral discs the laser channels were produced by a preliminarily blackened tip of the optical fibre, heated by the laser radiation ($\lambda = 0.97$ μm, $P = 3$ W). The total time of the laser setup operation in both cases amounted to ~5 min. As the channels were formed according to the technique of Ref. [2] the saline (the 0.9% aqueous solution of NaCl) was periodically injected into the disc via a puncture needle. The acoustic measurements in the course of the EVLA procedure were synchronously combined with the video record of the echogram from the ultrasound apparatus equipped with the linear ultrasound detector (7.5 MHz), using which the laser operation in veins was performed.

The optical registration of the processes was implemented using a Fastcam SA-3 camera (Photron, Japan) at a rate of 10000 frames per second. The power of optical radiations was controlled using a FieldMaster power meter with a LM-10HTD measuring head (Coherent, USA).

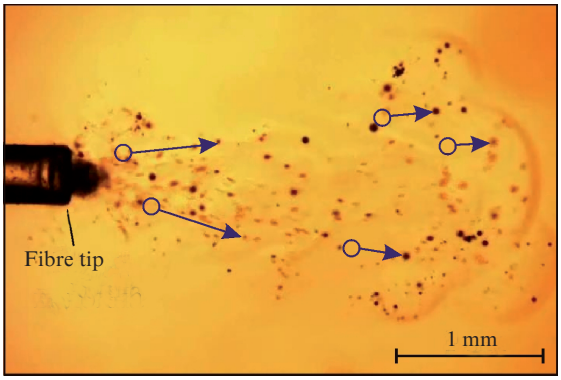

Figure 2. A frame of high-speed filming of vapour-gas bubbles at the fibre tip with an absorbing coating, merged in water, in the process of heterogeneous jet generation under the action of laser radiation (λ = 1.94 μm, P = 3 W). The circles mark the positions, where the microbubbles (pointed by arrows) have been located 8 ms ago.

3. Results

3.1. Laser-induced boiling of water

Figures 2 and 3 present the typical frames of rapid recording of laser-induced water boiling near the fibre tip in two regimes, the heterogeneous one with the blackened tip (Fig. 2) and the homogeneous one without the absorbing coating (Fig. 3). One can see that the boiling in these two regimes has different character. In the case of heterogeneous boiling (Fig. 2) at the heated tip of the fibre many small (the diameter 43 ± 19 μm) vapour-gas bubbles arise that form the string two-phase flow.

The scale of the produced hydrodynamic perturbations essentially exceeds the characteristic scale of the heater (the fibre tip diameter). The velocity of bubble motion near the tip amounts to ~80 mm s^{-1} and gradually decreases with distance from the tip. Simple counting of bubbles number in the course of frame-by-frame revision shows that during one second (3.2 ± 0.9) × 10^3 bubbles are generated on the fibre tip. In this case a weak dependence of the boiling intensity on the radiation wavelength is observed in the entire wavelength range (0.97–1.94 μm) studied. The generation of the two-phase jet flow is characterised by the power threshold and occurs only when $P \geqslant 3.2 \pm 0.3$ W. With the growth of power, the velocity of these jet flows near the working tip of the fibre monotonically increases from 85 ± 15 mm s^{-1} for $P = 3$ W to 450 ± 65 mm s^{-1} for P = 10 W. For below-threshold powers, the intense heterogeneous boiling at the fibre tip gradually ceases, and the motion of the liquid comes to the regime of free convection with the velocities below 0.5 mm s^{-1}. In this regime, the individual bubbles that appear at the heated tip from time to time tear off and emerge.

In the case of homogeneous boiling (Fig. 3), the large bubbles are quasi-periodically generated near the fibre tip. During ~100 μs they achieve their maximal size that amounts to 1.7 ± 0.8 mm (Fig. 3b and region 1 in Fig. 3c). Then, during nearly the same time, the bubbles collapse with subsequent expansion to 0.7 ± 0.4 mm (Fig. 3c). In the course of expansion the bubble simultaneously moves towards the free liquid (region 2 in Fig. 3c) with the velocity 28 ± 12 m s^{-1}. In Fig. 3c, the process of the bubble collapse and its consequent expansion are overlapped. Note that the homogeneous water boiling in water is observed only for the laser radiation with the wavelengths 1.56 and 1.94 μm, absorbed well in water.

The acoustic signals and spectrograms, corresponding to the regimes of heterogeneous and homogeneous boiling in water at the tip of the optical fibre also demonstrate significant qualitative differences (Fig. 4). In the first case (Fig. 2), the generation of continuous amplitude-modulated acoustic

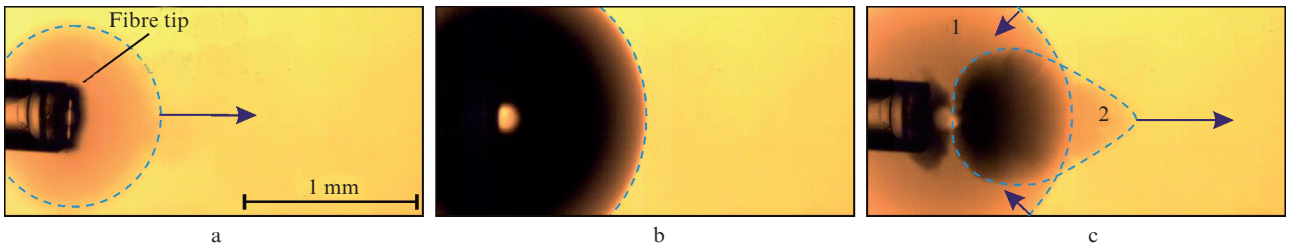

Figure 3. High-speed filming sequential frames (a, b, c) of a vapour-gas bubble near the fibre tip without an absorbing coating, merged in water, in the course of homogeneous boiling under the action of laser radiation (λ = 1.94 μm, P = 3 W). The time between the frames amounts to 100 μs. The dashed lines show the boundaries of the vapour-gas bubble, the arrows show the direction and velocity of its motion.

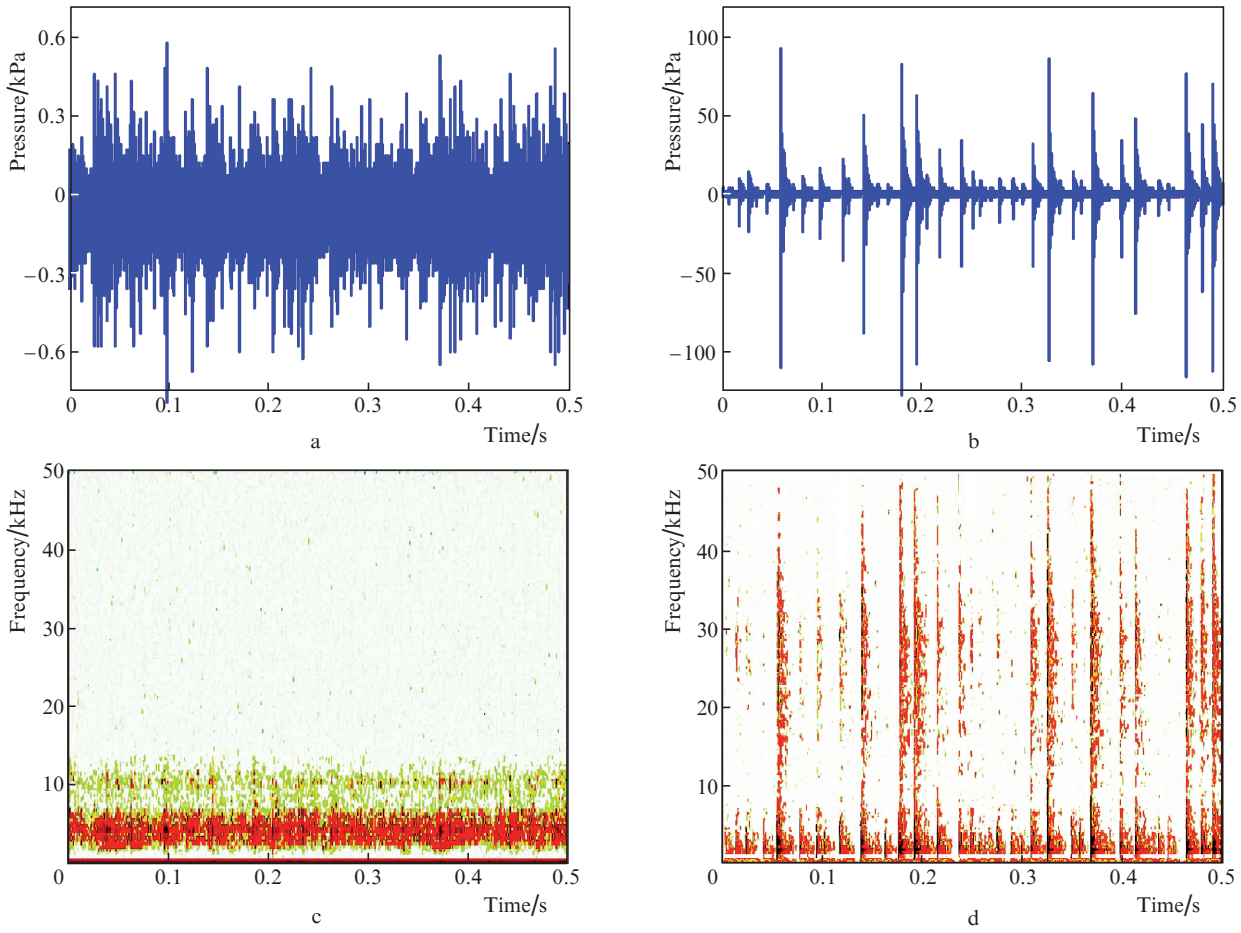

Figure 4. (a, b) Acoustic signals and (c, d) spectrograms of the signals, generated in the regimes of (a, c) heterogeneous boiling of water at the tip of the fibre with an absorbing coating and (b, d) homogeneous boiling in the case of the uncoated fibre tip; $\lambda = 1.94$ μm, $P = 3$ W.

signal occurs (Fig. 4a), the energy of which is concentrated in the range 1–12 kHz with the expressed maximum at 2–4 kHz (Fig. 4c). The homogeneous boiling (Fig. 3) gives rise to high-power relatively short decaying acoustic pulses (Fig 4b) that occupy the spectral range 0–50 kHz (Fig. 4d). The pulses are quasi-periodically repeated with the rate of 74 ± 9 Hz. Note that for homogeneous boiling the amplitude of pressure in the shock pulse (Fig. 4b) is by three orders of magnitude higher than in the case of heterogeneous boiling (Fig. 4a). Using the laser radiation with $\lambda = 1.56$ μm in the homogeneous boiling regime, similar shock pulses are also generated, but with significantly smaller repetition rate of 6.8 ± 1.9 Hz. Their maximal pressure amplitude, assessed using the needled hydrophone, was nearly similar for the radiations with $\lambda = 1.94$ and 1.56 μm and approached 1 MPa.

3.2. Laser-induced boiling of the liquid in an intervertebral disc

The analysis of the acoustic signal generated in the course of the formation of laser channels in the intervertebral disc in vitro has shown (Fig. 5) that the advance of the heated tip of the light-transporting fibre is accompanied with the generation of high-power relatively short damped acoustic pulses (Figs 5a and 5b). The pulses occupy the spectral range 0–10 kHz (Fig. 5c) and are repeated quasi-periodically with the rate 47 ± 9 Hz. Sometimes the generation of pulses with the repetition rate 107 ± 17 Hz occurs. Each of such pulsed signals [(*2*) in Fig. 5c] is accompanied by the bimodal precursor of essentially smaller amplitude [(*1*) in Fig. 5c], separated from the main pulse by 5 ± 2 ms.

Figure 6 shows the acoustic signal and its spectrogram, obtained during the execution of the laser treatment procedure in clinic [2], during which laser channels were produced in the nucleus pulposis of the disc with the blackened tip of the optical fibre heated by the laser radiation ($\lambda = 0.97$ μm, $P = 3$ W). In this case, the high-power relatively short damped acoustic pulses (Figs 6a and 6b) are generated that occupy the spectral range 0–6 kHz (Fig. 6b). In this case, one can select the signal regions, in which the pulses follow each other quasi-periodically with the rate 110 ± 20 Hz. Every acoustic pulse [(*2*) in Fig. 6c] is accompanied by the bimodal precursor [(*1*) in Fig. 6c] separated from the main pulse by 1.8 ± 0.6 ms.

3.3. Laser-induced boiling of liquid in a vein

Figure 7 presents the ultrasound (US) images and the acoustic signal, illustrating the processes of laser-induced boiling of blood in a vein in the course of executing the EVLA procedure. From the US images (Figs 7a, 7b and 7d) one can see that at the initial moment of laser exposure, a large (the diameter $D \sim 7$ mm) vapour-gas bubble is formed. Because of the strong shielding only the upper boundary of this bubble is seen in the US image (Figs 7b and 7d). Its appearance at the

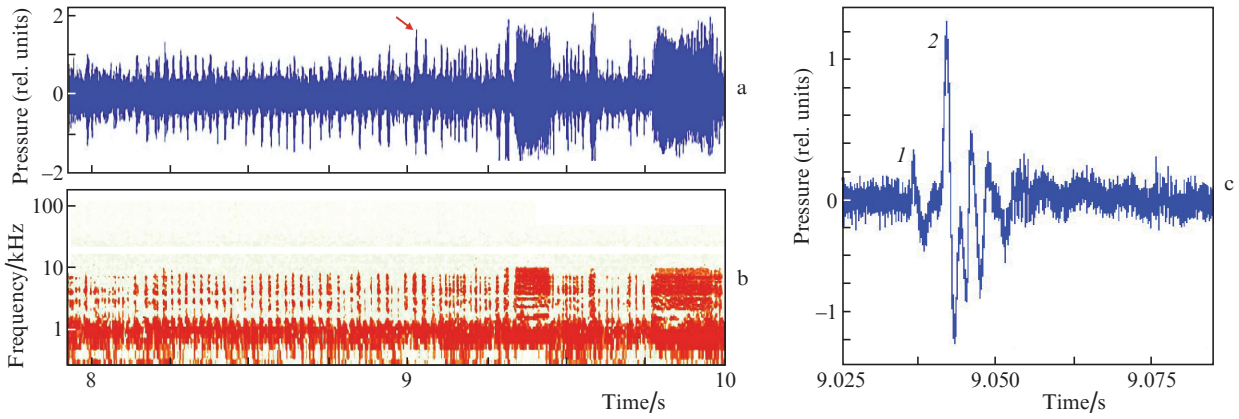

Figure 5. (a) Fragment and (b) spectrogram of the acoustic signal generated in the course of moving the fibre in the intervertebral disc, as well as (c) the detailed record of the signal segment, marked by arrow in Fig. 5a [(*1*) precursor; (*2*) the first pressure pulse]. The fibre tip is blackened, λ = 0.97 μm, P = 3 W.

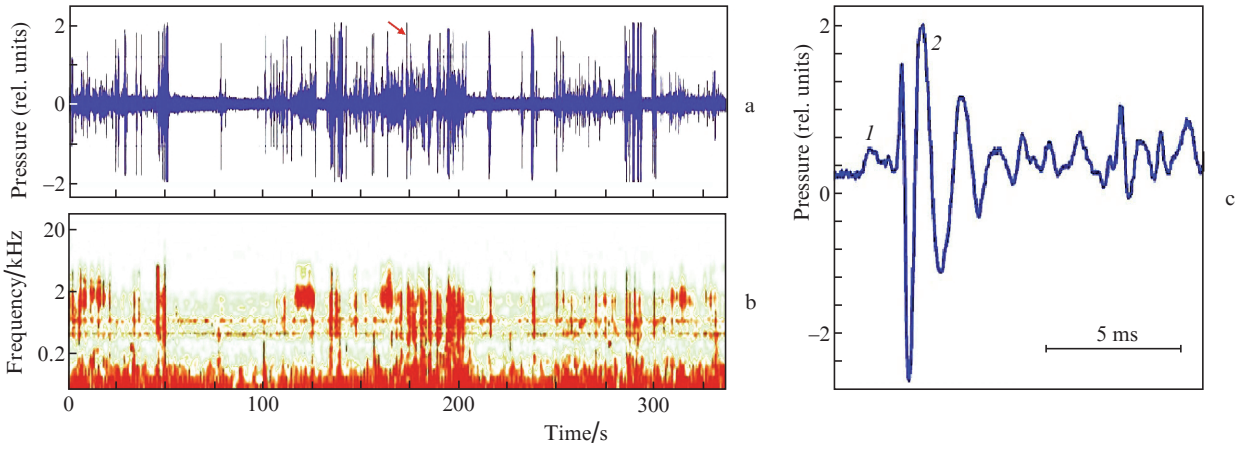

Figure 6. (a) Fragment and (b) spectrogram of the acoustic signal generated in the intervertebral disc with the fibre motion in the course of the clinical procedure [2], as well as (c) the detailed record of the signal fragment, marked by the arrow in Fig. 6a [(*1*) precursor; (*2*) the maximal pressure pulse]. The fibre tip is blackened, λ = 0.97 μm, P = 3 W.

initial time of the laser radiation impact is accompanied by the generation of a high-power acoustic signal in the form of a few damped oscillations with the frequency ~1 kHz and the steep rising edge (Fig. 7e). Immediately after these high-power oscillations, the continuous amplitude-modulated acoustic signal with the frequency 1–3 kHz is generated. Simultaneously with the generation of the large vapour-gas bubble, the two-phase jet flow appears, distinctly seen at the distances up to ~13 mm from the fibre tip [(*3*) in Fig. 7b]. The analysis of sequential US images allowed the determination of the velocity of the two-phase jets, consisting of bubbles with the dimension 100–500 μm that approaches 75 mm s^{-1} at the fibre tip and decreases with distance. In the US image obtained in 10 s after the beginning of laser exposure, the jet flow propagates in the vein to the distance to ~35 mm from the tip [(*3*) in Fig. 7c].

3.4. Laser-induced boiling of liquid in cysts

The characteristic US images, obtained in the course of laser clinical procedures and illustrating the features of laser-induced boiling in Baker's and mammary gland cysts, are presented in Fig. 8. The preliminarily blackened tip of the optical fibre is heated by the laser radiation, which leads to the heterogeneous boiling of the cystous liquid (Figs 8b and 8d). In the case of a Baker's cyst, the regime of free convection is implemented with the velocity ~0.5 mm s^{-1}. The bubbles that appear at the fibre tip emerge and accumulate in the upper part of the cystous cavity [(*3*) in Fig. 8b]. On the contrary, the laser-induced boiling of the cystous liquid in the mammary gland leads to the heterogeneous stream generation of vapour-gas bubbles near the fibre tip with the velocity ~5 mm s [(*3*) in Fig. 8b]. In this case, the bubbles accumulate mainly at the side of the cyst, opposite to the fibre tip.

4. Discussion

Above we considered the laser-induced effects in biological media (great saphenous vein, intervertebral disc, mammary gland cyst, and Baker's cyst), caused by the continuous laser heating in two boiling regimes, the heterogeneous boiling at the surface of the fibre tip coated with the absorber, and the heterogeneous boiling that occurs in the course of laser radiation propagation through the absorbing liquid. The used intensities of laser radiation did not exceed 10^4 W cm^{-2}, which is by four orders of magnitude lower than the inten-

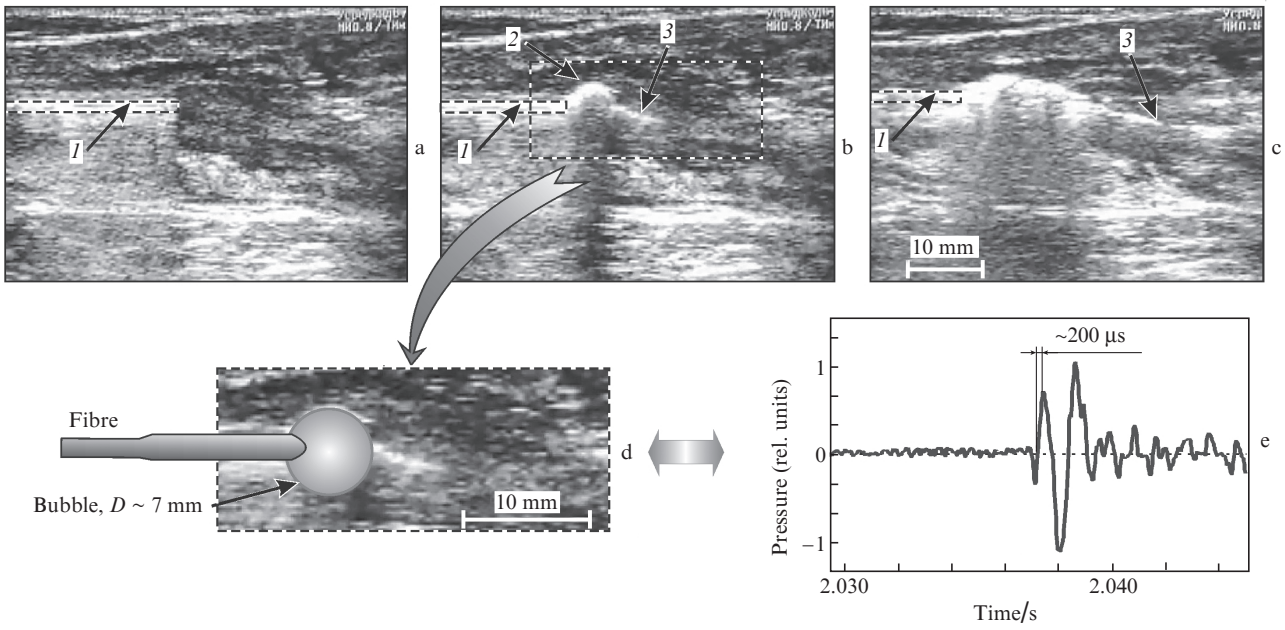

Figure 7. Ultrasound images (a) before the laser impact, (b, d) at the initial moment and (c) in 10 s after it, illustrating the processes of laser-induced boiling of blood in a vein in the course of EVLA procedure, as well as the acoustic signal, recorded at the initial moment (b, d) of the laser impact due to the generation of the bubble with D ~ 7 mm (the time after switching the laser on is 200 μs) (e); (*1*) laser fibre, (*2*) the upper boundary of the vapour-gas bubble, (*3*) two-phase jet flow. Inset (d) schematically shows the laser fibre without an absorbing coating with a bubble on the tip; λ = 1.47 μm, P = 8.5 W.

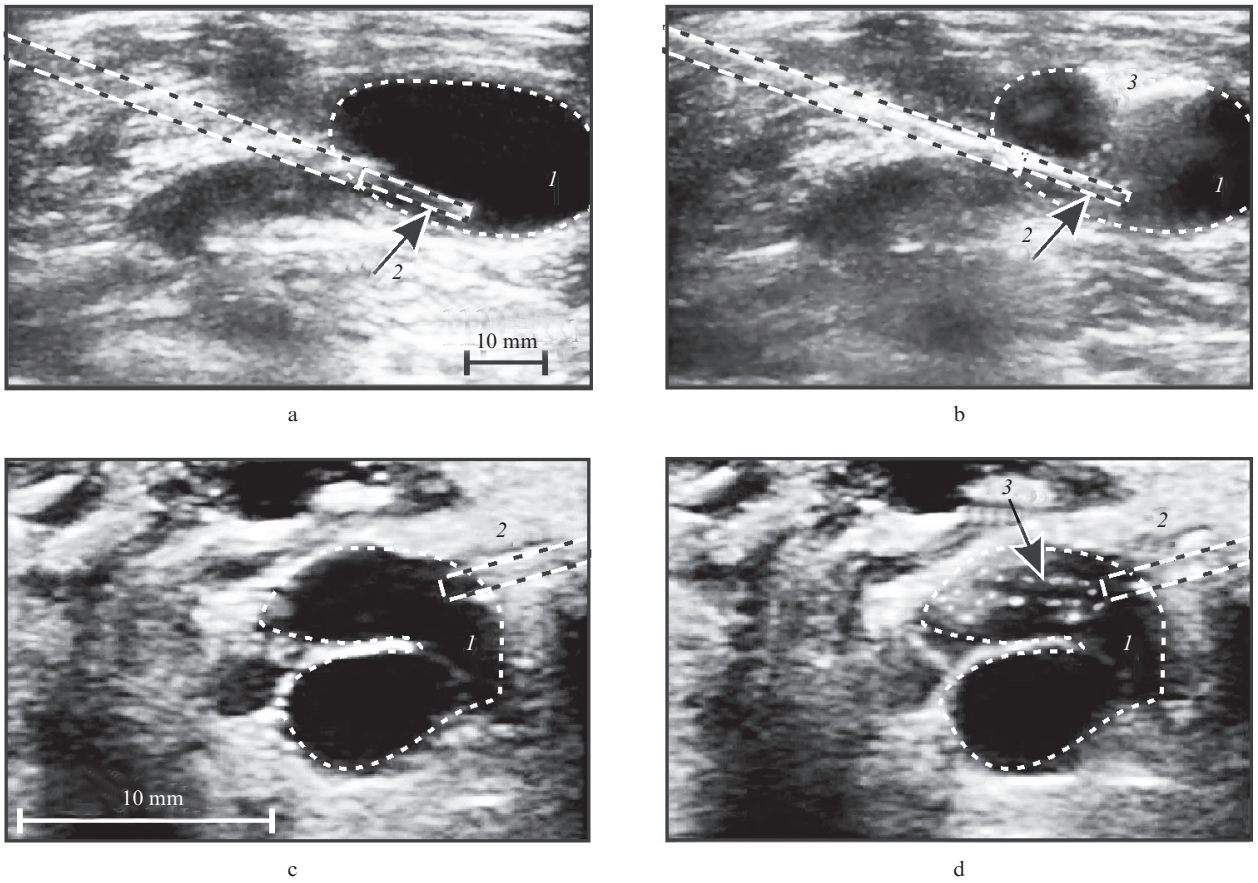

Figure 8. Ultrasound images illustrating the laser-induced heterogeneous boiling in the Baker's cyst (a) before and (b) at the moment of laser action, P = 2 W; in the mammary gland cyst (c) before and (d) at the moment of laser action, P = 5 W; (*1*) cyst, (*2*) laser fibre, (*3*) vapour-gas bubbles (the fibre tip is blackened, λ = 0.97 μm).

sity of optical breakdown [39]. The laser radiation wavelengths lied in the near infrared range (0.97–1.94 μm). In this range, the main biotissue chromophores are the pigments (in the short-wavelength part of the range) and water (in the long-wavelength part) [40].

4.1. Laser-induced boiling of water

In the case of heterogeneous boiling (Fig. 2), the directional jet flows of liquid with bubbles are observed with the velocity up to ~80 mm s^{-1} near the fibre tip. A large number of tiny vapour-gas bubbles having the diameter to 60 μm is formed on the tip. This boiling is accompanied by the generation of continuous amplitude-modulated acoustic signal (Fig. 4a) with the energy mainly concentrated within the frequency range 2–4 kHz (Fig. 4c). This regime has all features of superintensive bubble boiling [17]: i) the large value of the specific heat flow (2.4×10^3 W cm^{-2} for $P = 3$ W, and 8×10^3 W cm^{-2} for $P = 10$ W); ii) the characteristic acoustic effects; iii) the scale of hydrodynamic perturbation exceeding that of the heater; and iv) the critical power dependence of the regime initiation (with the threshold power amounting to 3.2 ± 0.3 W). We suppose that the nature of the recorded spectral maximum (2–4 kHz) in the case of heterogeneous boiling is related to the rate of bubble production at the fibre tip [$(3.2 \pm 0.9) \times 10^3$ s^{-1}]. The similar conclusion was made in Ref. [41], where the generation of the acoustic signal in water was studied using a fibre converter of laser radiation.

It is known that the character of boiling in an underheated liquid below the saturation temperature depends on the value of the heater surface overheating ΔT relative to the saturation temperature [14–18]. The estimates obtained with microheaters [17] show that in the water free of bubbles at $\Delta T > 25$ °C the magnitude of the specific flux from the heater $\boldsymbol{q}$ (in kW cm^{-2}) in the case of superintensive bubble boiling is linearly related to ΔT (in °C):

$$\Delta T = (\boldsymbol{q} + 0.87)/0.04. \quad (1)$$

Since the laser-induced heterogeneous stream boiling (Fig. 2) is superintensive bubble boiling [17], expression (1) can be used to assess the overheating ΔT at the tip of the laser fibre. For the laser fibre diameter 400 μm and $P = 3$ W (Fig. 2), the specific flux is $\boldsymbol{q} = P/S = 2.4$ kW cm^{-2} (S is the tip area), and according to (1) the overheating of the tip with respect to the water saturation temperature (100 °C) amounts to 81°C. Note that this estimate is made assuming that the coating at the fibre tip absorbs 100% of the incident power. Such great overheating leads to the heterogeneous boiling that produces a large number of rapidly growing bubbles [$(3.2 \pm 0.9) \times 10^3$ s^{-1} at $P = 3$ W] in the microscopic caverns of the absorbing coating surface. In our opinion, the integral momentum received by the water molecules in the course of bubble production and directed from the tip is transferred to the overheated water and leads to the formation of two-phase jet flows of the heated liquid [27]. The bubbles initially moving off the working fibre tip surrounded by water having the mean temperature of vapour-gas mixture ~180 °C rapidly increase their size because of the high pressure of the vapour (~8×10^5 Pa), intense evaporation and release of gas dissolved in the water. As a result of the evaporation and cooling processes in the course of mixing with the underheated liquid he temperature of vapour in the bubbles first decreases to the equilibrium one at the atmospheric pressure (~100 °C). The estimates show that in the composition of vapour-gas bubbles at the temperature 100 °C the fraction of water vapour amounts to ~50%. If there were no gas in the bubble, then, according to [42], it would collapse during the time

$$t_c = 0.915 R_{max} \sqrt{\frac{\rho}{p_0 - p_v}}, \quad (2)$$

where R_{max} is the maximal radius of the bubble; ρ is the density of water; p_0 is the external pressure (~100 kPa); p_v is the saturation vapour pressure (2.33 kPa at 20 °C). According to Eqn (2), the vapour bubble with $R_{max} = 60$ μm (Fig. 2) would collapse in $t_c \approx 3$ μs.

With further removal from the working tip, the temperature of vapour-gas-liquid jets gradually decreases to the temperature of the underheated liquid in the volume. At considerable underheating (the temperature ~63 °C for biological liquids) the bubbles far from the fibre tip can be considered consisting of gas [27]. In our opinion, in addition to the release of the dissolved gas from the heated water volume, the gas in the bubbles can appear due to the processes of carbon oxidation at the fibre tip.

In the case of homogeneous boiling the large vapour-gas bubbles quasi-periodically arise and collapse near the fibre tip (Fig. 3). This process is accompanied by the generation of high-power relatively short damped acoustic pulses (Fig. 4b), occupying the spectral range 0–50 kHz (Fig. 4d) and repeated quasi-periodically with the rate 74 ± 9 Hz. Such a shock signal manifests itself in the spectrograms as distinct narrow vertical frequency-elongated stripes (Fig. 4c), which allow the differentiation between the shock processes and the shockless ones. The analysis of the optical images (Fig. 3) and the acoustic signals (Fig. 3 and Figs 4b and 4d) allows the conclusion that the formation of a bubble and the generation of sound under the action of continuous-wave laser radiation develop according to the thermocavitation mechanism [22]. First, due to the absorption of laser radiation in water, the overheated region is gradually formed near the fibre tip. After the achievement of the near-spinodal temperature (T_C ~ 305 °C for the atmospheric pressure [43]) the explosive boiling with the formation of rapidly expanding bubble occurs due to fluctuations. On achieving the maximal size the bubble collapses just as rapidly (Fig. 3) and then expands again (but to a smaller size) and simultaneously moves from the tip towards the free liquid. As a result of such process, the liquid in front of the working tip of the optical fibre is replaced with the new one, and with its heating a new cycle begins. According to [44], the frequency of the bubble free oscillations is expressed as

$$F \approx \frac{1}{2\pi R}\left(\frac{3\gamma p_0}{\rho}\right)^{1/2}, \quad (3)$$

where γ is the ratio of specific heat capacities for the gas in the bubble. For the torn-off bubble with the radius $R = 0.35 \pm 0.2$ mm (Fig. 3) for $\gamma = 1.4$, $\rho = 10^3$ kg m^{-3} and $p_0 \approx 100$ kPa we obtain $F \sim 10$ kHz.

The repetition rate of the thermocavitation cycles is determined by the rate of the liquid heating near the tip, which is proportional to the intensity and the absorption coefficient of laser radiation. In the case of using the radiation with $\lambda = 1.94$ μm efficiently absorbed in water at $P = 3$ W (the specific flux $\boldsymbol{q} = 2.4$ kW cm^{-2}) this rate amounts to 74 ± 9 Hz.

4.2. Laser-induced boiling of liquid in intervertebral disc

The results obtained in the experiments with water allowed the specification of the mechanism of laser impact on the biotissues in vitro and the tissues of the organism in vivo subjected to laser surgery manipulations. Thus, the acoustic studies, performed during the laser formation of channels in an intervertebral disc with the addition of aqueous solutions in vitro and in vivo following the technique [2], have shown that both the acoustic signals and their spectra (Figs 5a and 5c; Figs 6a and 6c) are qualitatively very much the same as the results for the homogeneous boiling of water (Figs 4b and 4d). The presence of distinct narrow vertical frequency elongated stripes in the spectrograms (Fig 5b; Fig. 6b) shows that the shock processes periodically occur in the tissues of the disc nucleus pulposis as the heated tip of the laser fibre moves in. We believe that the cause of these processes is the heterogeneous explosive boiling of the liquid in the microscopic caverns of the absorbing coating of the fibre and in microcavities of the nucleus pulposis of the intervertebral disc near the fibre tip tightly pressed to the tissue [34]. In fact, the formation of expanding bubbles during such boiling is implemented via the thermocavitation mechanism [9] and, in contrast to the case of free water (Fig. 3), occurs in the closed microscopic volumes. The pressures that appear in these volumes under fast heating of water (1.6 MPa at the temperature 200 °C and already as much as 4 MP at 250 °C) lead to the tearing of the disc tissue that facilitates the efficient formation of laser channel with the velocity 1–3 mm s^{-1} [2, 12]. The sufficiently rigorous periodicity of these processes found in this case is, probably, related to the appearance of resonancely amplified self-oscillations [25–26] under the conditions of the acoustic resonator having the sufficiently high Q-factor [13], which is the intervertebral disc. Note that in the process of channel formation in the biotissue near the fibre tip the sufficiently high pressure is developed (~1 MPa at the pressure force of 1 N acting on the fibre), which leads to the significant reduction of the size of the new phase nuclei and the development of boiling in the microscopic volumes. Both these factors make the maximal temperature of the liquid laser heating T_{max} closer to the spinodal temperature T_C, and at $T_{max} > 0.7T_C$ the explosive boiling of water occurs [43].

Thus, it is established that in the course of laser channel formation in a biotissue (intervertebral disc) the shock processes periodically occur, which are related to the explosive water boiling near the fibre tip that leads to the tissue tearing. We believe that the broadband acoustic oscillations generated in this case trigger the disc tissue regeneration caused by the effects of mechanobiology [12, 35].

4.3. Laser-induced boiling of liquid in vein

The analysis of US images and accompanying acoustic signals, observed in the course of laser surgical treatment of varicose veins, provided new information about the EVLA mechanism. From the comparison of US images (Figs 7a, 7b and 7d) it is seen that at the initial moment of laser exposure a big bubble having the diameter of ~7 mm is rapidly formed near the uncoated fibre tip. Its appearance is accompanied by the generation of a high-power acoustic signal (Fig. 7e) in the form of a few damped oscillations with the frequency ~1 kHz and the steep rising edge having the duration ~200 μs. Such an acoustic signal qualitatively corresponds to the results, obtained in the case of homogeneous water boiling (Figs 4b and 4d). This fact allows a conclusion that at the third second of laser operation a large vapour-gas bubble is explosively produced (Fig. 7d) via the thermocavitation mechanism [22], accompanied by the acoustic signal generation (Fig. 7e). Initially, thanks to the strong absorption of the laser radiation with $\lambda = 1.47$ μm by water, an overheated region is formed near the fibre tip. Then the explosive boiling of the liquid occurs with the formation of rapidly expanding vapour-gas bubble. At the initial moment determined by the rising edge of the pressure, having the duration ~200 μs, the vapour-gas bubble expands very rapidly. Then, at the moment corresponding to the minimal pressure (Fig. 7d), it achieves its maximal size and the rate of its wall expansion decreases to zero. The mean rate of bubble expansion is easily estimated using its maximal radius (~3.5 mm) and the time of expansion (~0.85 ms) and amounts to ~4 m s^{-1}.

The potential energy E of the formed bubble is determined by its maximal radius R_{max} and the difference of hydrostatic pressure p_0 and the vapour pressure inside the bubble p_v [45]

$$E = \frac{4\pi}{3}(p_0 - p_v)R_{max}^3. \quad (4)$$

For the bubble with $R_{max} = 3.5$ mm, like in Fig. 7, according to Eqn (4) the potential energy $E \approx 17$ mJ, which is by three orders of magnitude smaller than the energy absorbed during 2 s (17 J). This means that practically all energy is spent for blood heating, generation of mechanical oscillations and jet formation.

In the case of EVLA the heating of intravenous liquid to the temperatures sufficient for thermocavitation requires a little more than 2 s of laser exposure (Fig. 7e), which is much longer than the period between the individual thermocavitation process (14 ± 2 ms) in the course of homogeneous boiling of water (Fig. 4b). This difference is explained by the essentially smaller intensity of laser radiation acting on the blood, which is due to larger diameter of the fibre used for EVLA (3.7 mm instead of 0.4 mm) and wider directional pattern, providing the radial exit of laser radiation. Moreover, in the case of EVLA the effective heated volume of the liquid increases due to the triple reduction of the absorption coefficient (from 92 cm^{-1} at $\lambda = 1.94$ μm to 30 cm^{-1} at $\lambda = 1.47$ μm).

Simultaneously with the bubble generation the two-phase jet flow appears in the vein [(*3*) in Fig. 7b] with the bubbles having the diameter 100–500 μm, moving near the fibre tip with the velocity ~75 mm s^{-1}. Such flows can propagate in the vein to the distance approaching 35 mm from the tip of the laser fibre [(*3*) in Fig. 7c]. Note that the bubbles in the jet flows at a small distance from the fibre tip are surrounded by the liquid having the temperature exceeding the saturation temperature (~100 °C) and are vapour-gas ones, with the density of water vapour higher than 0.6 kg m^{-3}. However, at significant distances they become purely gas-containing ones, since the blood temperature here amounts to ~37 °C and all the vapour is condensed. As shown by the experiments with water (Section 3.1), such jet flows arise as a result of the heterogeneous boiling and are accompanied by the acoustic signal generation (Fig. 4a) in the spectral region 2–4 kHz (Fig. 4c). We suppose that the signal in the frequency range 1–3 kHz (Fig. 7e), observed immediately after the high-power thermocavitation oscillations, corresponds to the detected two-phase jet flow in the vein [(*3*) in Fig. 7c]. Thus, in the

course of laser surgical treatment of varicose veins the thermal impact on the vein walls occurs due to the laser-induced homogeneous and heterogeneous boiling of blood.

4.4. Laser-induced boiling of liquid in cysts

The analysis of characteristic US images (Fig. 8) obtained in clinic in the course of laser procedures in Baker's cyst and mammary gland cyst has shown that in this case the heterogeneous boiling of liquid takes place (Figs 8b and 8d). In the case of the Baker's cyst at the power $P = 2$ W (below the threshold ~3 W) the free convection regime is implemented with sufficiently small velocities (~0.5 mm s^{-1}). The bubbles surrounded by the heated liquid emerge and accumulate in the upper part of the cystous cavity [(*3*) in Fig. 8b]. In the case of the mammary gland cyst, the laser power $P = 5$ W exceeds the threshold of jet boiling, which leads to the heterogeneous generation of a jet of vapour-gas bubbles near the fibre tip [(*3*) in Fig. 8d] with the velocity ~5 mm s^{-1}. In this case, the cystous liquid with vapour-gas bubbles heated at the working tip accumulates mainly at the opposite cyst wall, efficiently heating it. Thus, during the laser procedures in a Baker's cyst and mammary gland cyst the heat impact is transferred to the wall due to the laser-induced heterogeneous boiling. On exceeding the threshold power (Fig. 8d) the superintensive bubble boiling is observed [17, 46], which enhances the therapeutic efficiency.

5. Conclusions

In the present paper we have studied the thermal and transport processes caused by the boiling of biological liquids exposed to the continuous-wave near-IR laser radiation of moderate power, delivered by means of an optical fibre. Such processes are implemented during the execution of a few particular clinical procedures, aimed at modifying (veins), removal of pathological growths (mammary gland cyst and Baker's cyst), and tissue regeneration (intervertebral discs).

It is shown that in these cases two main regimes of boiling take place in water and biological liquids, namely, the heterogeneous jet boiling at the heated surface of the blackened tip of the fibre, and the homogeneous boiling, when the laser radiation is efficiently absorbed in the liquid volume near the fibre tip. It is found that the heterogeneous jet boiling at laser powers above the threshold of two-phase jet generation (3.2 ± 0.3 W for water) is actually superintensive bubble boiling. The domination of a particular boiling regime depends on the presence of absorbing coating at the fibre tip, on the tissue type, as well as on its shape (e.g., the presence of cavities or channels in the tissue). Both regimes of boiling (heterogeneous and homogeneous) provide high values of specific heat flux.

Note that in the proposed approach the modification and destruction of biotissues occur due to the fast delivery of heat by the two-phase jet flows of liquid, formed due to its boiling, rather than the direct laser heating. This simultaneously provides the high rate of heat delivery to the pathological biotissue, excludes its overheating (the temperatures significantly exceeding 100 °C), as well as the undesired eating of the adjacent tissues. The results of the performed studies allow the optimization of medical technologies, based on the use of moderate-power firbe lasers of near-IR range, which find wider and wider application in medical practice.

Acknowledgements. The work was supported by the Russian Science Foundation (Grant No. 14-25-00055).

References

1. Sandler B.I., Sulyandziga L.N., Chudnovskii V.M., Yusupov V.I., et al. *Perspektivy lecheniya diskogennykh kompressionykh form poyasnichno-kresttsovykh radikulitov s pomoshchyu punktsionnykh neendoskopicheskikh lazernykh operatsii* (Prospects of Treatment of Discogenic Compression Forms of Lumbosacral Radiculitis Using Percutaneous Non-Endoscopic Laser Operations) (Vladivostok: Dal'nauka, 2004) p. 181.
2. Minaev V.P. *Quantum Electron*., **35** (11), 976 (2005) [*Kvantovaya Elektron*., **35** (11), 976 (2005)].
3. Proebstle T.M., Lehr H.A., Kargl A., Espinola-Klein C., Rother W., Bethge S., Knop J. *J. Vascular Surgery*, **35**(4), 729 (2002).
4. Altshuler G.B., Erofeev A.V., Yaroslavsky I. US Patent No. 6, 723, 090 (2004).
5. Krochek I.V., Privalov V.A., Lappa A.V., Evnevich M.V., Minaev V.P. *Lazernaya osteoperforatsiya v lechenii ostrogo i khronicheskogo osteomielita. Metodicheskiye rekomendatsii* (Laser Osteoperforation in the Treatment of Acute and Chronic Osteomyelitis. Methodic Recommendations) (Chelyabinsk: ChGMA, ChGU, 2004).
6. Minaev V.P. *Almanakh Klinicheskoi Meditsiny*, **17** (2), 116 (2008).
7. Bagratashvili V.N., Sobol' E.N., Shekhter A.B. *Lazernaya inzheneriya khryashchei* (Laser Engineering of Cartilages) (Moscow: Fizmatlit, 2006).
8. Yamamoto T., Sakata M. *J. Vascular Surgery: Venous and Lymphatic Disorders*, **2** (1), 61 (2014).
9. Vogel A., Venugopalan V. *Chem. Rev*., **103** (2), 577 (2003).
10. Chudnovskii V.M., Yusupov V.I., Zakharkina O.L., Ignatyeva N.Yu., Zhigar'kov V.S., Yashkin M.N., Bagratashvili V.N. *Sovremennye Tekhnologii v Meditsine*, **8** (2), 6 (2016).
11. Yusupov V.I., Chudnovskii V.M., Bagratashvili V.N. *Laser Phys*., **21** (7), 1230 (2011).
12. Yusupov V.I., Chudnovskii V.M., Bagratashvili V.N., in *Hydrodynamics – Advanced Topics* (InTech, 2011) p. 95; https://doi.org/10.5772/28517.
13. Chudnovskii V., Bulanov V., Yusupov V. *Fotonika*, **1**, 30 (2010).
14. Nesis E.I. *Kipenie zhidkostei* (Boiling of Liquids) (Moscow: Nauka, 1973) p. 280.
15. Dhir V.K. *Ann. Rev. Fluid Mechanics*, **30** (1), 365 (1998).
16. Kutateladze S.S. *Osnovy teorii teploobmena* (Fundamentals of Heat Exchange Theory) (Moscow: Atomizdat, 1979).
17. Zhukov S.A., Afanas'ev S.Yu., Echmaev S.B. *Int. J. Heat Mass Transfer*, **46**, 3411 (2003).
18. Tong L.S., Tang Y.S. *Boiling Heat Transfer and Two-Phase Flow* (Washington: CRC Press., Taylor & Francis, 1997).
19. Zeigarnik Yu.A., Platonov D.N., Khodakov K.A., Shekhter Yu.L. *High Temp.*, **50** (1), 78 (2012).
20. Rastopov S.F., Sukhodol'skii A.T. *Sov. Phys. Dokl*., **32** (8), 671 (1987) [*Dokl. Akad. Nauk SSSR*, **295**, 1104 (1987)].
21. Yusupov V.I., Konovalov A.N., Ulyanov V.A., Bagratashvili V.N. *Acoust. Phys.*, **62** (5), 537 (2016) [*Akust. Zh.*, **62** (5), 531 (2016)].
22. Rastopov S.F., Sukhodolsky A.T. *Proc. SPIE*, **1440**, 127 (1990).
23. Rastopov S.F., Sukhodolsky A.T. *Phys. Lett. A*, **149**, 229 (1990).
24. Padilla-Martinez J.P., Berrospe-Rodriguez C., Aguilar G., Ramirez-San-Juan J.C., Ramos-Garcia R. *Phys. Fluids*, **26**, 122007 (2014); https://doi.org/10.1063/1.4904718.
25. Dorofeev B.M. *High Temp*., **23** (3), 479 (1985) [*Teplofiz. Vysok. Temp*., **23**, 586 (1985)].
26. Dorofeev B.M., Volkova V.I. *Acoust. Phys*., **54**, 633 (2008).
27. Yusupov V.I., Chudnovskii V.M., Bagratashvili V.N. *Laser Phys*., **20** (7), 1641 (2010).
28. Feras Marqa M., Mordon S., Betrouni N. *Las. Surgery Med*., **44**, 832 (2012).
29. Belikov A.V., Skripnik A.V., Kurnyshev V.Yu., Shatilova K.V. *Quantum Electron*., **46** (6), 534 (2016) [*Kvantovaya Elektron*., **46** (6), 534 (2016)].

30. Pimentel-Dominguez R., Hernández-Cordero J., in *Experimental and Theoretical Advances in Fluid Dynamics, Environmental Science and Engineering* (Berlin, Heidelberg: Springer-Verlag, 2012); https://doi.org/10.1007/978-3-642-17958-7_32.
31. Kukhareva L.I., Nevozhay V.I., Chudnovskii V.M. *Dal'nevostochnyi Meditsinskii Zhurnal*, **3**, 49 (2008).
32. Anufrieva S.S., Bordunovskii V.N., Kurenkov E.L. *Vestnik YuUrGU*, **19**, 43 (2010).
33. Vuylsteke M.E., Mordon S.R. *Ann. Vascular Surgery*, **26** (3), 424 (2012).
34. Chudnovskii V.M., Yusupov V.I., Makhovskaya T.G. *Vestnik Nevrologii, Psikhiatrii i Neyrokhirurgii*, **4**, 76 (2013).
35. Yusupov V.I., Bulanov V.V., Chudnovskii V.M., Bagratashvili V.N. *Laser Phys*., **24** (1), 015601 (2014); https://doi.org/10.1088/1054-660X/24/1/015601.
36. Stoltz J.F. *Mechanobiology: Cartilage and Chondrocyte* (Amsterdam, Netherlands: Ios Press, 2000).
37. Bagratashvili V.N., Zapharkina O.L., Ignatyeva N.Yu., Lunin V.V. *Lezerno-indutsirovannaya i termicheskaya modifikatsiya struktury soyedinitel'nykh tkaney* (Laser-Induced and Thermal Modification of Connective Tissues) (Dolgoprudnyi: Intellekt, 2016) p. 208.
38. Deng R., He Y., Qin Y., Chen Q., Chen L. *Yaogan Xuebao – J. Remote Sensing*, **16**, 192 (2012).
39. Lyamshev L.M. *Sov. Phys. Usp*., **30** (3), 252 (1987) [*Usp. Fiz. Nauk*, **151** (3), 479 (1987)].
40. Downing H.D., Williams D.J. *Geophys. Res*., **80**, 1656 (1975).
41. Skripnik A.V. *Izv. Vyssh. Uchebn. Zaved., Ser. Priborostroyeniye*, **58** (5), 385 (2015).
42. Keller J.B., Miksis M. *J. Acoust. Soc. Am*., **68** (2), 628 (1980).
43. Skripov V.P., Sinitsyn E.N., Pavlov P.A., Ermakov G.V., Muratov G.N., Bulanov N.V., Baidakov V.G. *Thermophysical Properties of Liquids in the Metastable (Superheated) State* (New York: Gordon and Breach Sci. Publ., 1988).
44. Minnaert M. *Philos. Mag*., **16**, 235 (1933).
45. Brennen C.E. *Cavitation and Bubble Dynamics* (New York: Oxford University, 1995).
46. Chudnovskii V.M., Yusupov V.I., Zhukov S.A., Echmaev S.B., Bagratashvili V.N. *Dokl. Akad. Nauk*, **473** (5), 533 (2017).